Consistent Twu parameters for more than 2500 pure fluids from critically evaluated experimental data[†]

Ian H. Bell,[*,‡] Marco Satyro,[¶] and Eric W. Lemmon[‡]

‡*National Institute of Standards and Technology, Boulder, CO, USA*
¶*Formerly of Virtual Materials Group Inc.*

E-mail: ian.bell@nist.gov

Abstract

The construction of the standard cubic equations of state such as Peng-Robinson or Soave-Redlich-Kwong does not automatically yield physically reasonable values when the equation of state is extrapolated beyond the range where experimental data are available. A multi-property fitting exercise was carried out in which we obtained a consistent set of Twu α function parameters for 2570 pure fluids based on the experimental data contained in the ThermoDataEngine (TDE) database developed at NIST. We have applied the consistency checks of Le Guennec *et al.* to the Twu α function of the Peng-Robinson equation of state. The experimental data stored in TDE passed through a critical evaluation, and we used only the data that were determined to be thermodynamically reliable. Over all the considered fluids, the mean average percentage error is approximately 7% for vapor pressure, 1% for latent heat of vaporization, and 1% for saturation specific heat. Comprehensive supplemental materials with the complete set of analytic derivatives, the obtained parameters, and the fitting code in C++, is provided.

1 Introduction

Cubic equations of state (EOS) have a pedigree dating back to the work of van der Waals in 1873.[1] In spite of their well-documented deficiencies described by for instance Trebble and Bishnoi[2] or Boshkova and Deiters,[3] cubic EOS retain a prominent place in chemical engineering (and many other fields) thanks to their simplicity. Though much more accurate multiparameter fundamental equations of state are available in thermophysical property libraries, cubic equations of state show no signs of falling into disuse.

One of the well-documented challenges with cubic equations of state is their relatively poor predictions of thermodynamic properties (e.g., the vapor pressures of polar fluids like water) when generalized estimation schemes are employed for the attractive parameters in the equation of state, such as in the conventional Peng-Robinson equation of state.[4,5] When the attractive parameters are fit to experimental data, as in this work, the equation of state can yield much better predictions of thermodynamic properties. Figure 1 gives a graphical representation of the problem. This figure shows that at low reduced temperatures,

[†]Commercial equipment, instruments, or materials are identified only in order to adequately specify certain procedures. In no case does such identification imply recommendation or endorsement by the National Institute of Standards and Technology, nor does it imply that the products identified are necessarily the best available for the purpose. Contribution of the National Institute of Standards and Technology, not subject to copyright in the US

the errors in vapor pressure prediction from the conventional Peng-Robinson equation are more than 20% as compared to the reference equation of state of Wagner and Pruß[6]! The common "solution" to this problem is to introduce empiricism, or adjustable parameters that must be fit by the correlator.

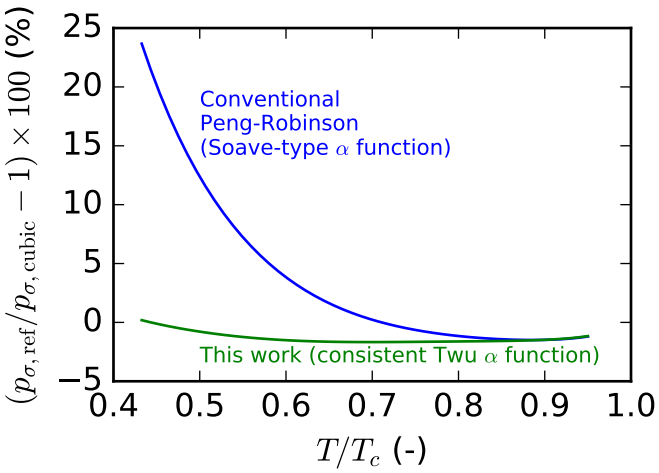

Figure 1: Error in the prediction of the vapor pressure of water from the default Peng-Robinson α function with the α function from this work. The subscript "ref" refers to the reference multiparameter equation of state of Wagner and Pruß[6]

In the literature there have been a few groups that have published large libraries of these adjustable parameters for cubic equations of state. The most significant recent contributions have been those of Horstmann *et al.*[7] and Le Guennec *et al.*[8] In particular the work of Le Guennec *et al.* is important here because their library of adjustable parameters were obtained according to a set of rigorous consistency checks, the same checks applied here.

While the overall aim of this work is similar to that of Le Guennec *et al.*, we made some improvements to the fitting procedure:

- *More comprehensive set of pure fluids*: In Le Guennec *et al.*, the DIPPR database was used to generate pseudo-experimental data points for 1197 pure fluids for which vapor pressure, latent heat, or saturation specific heat data were available. In this work we used the ThermoDataEngine (TDE) database of NIST, which provides data coverage for more than 23,000 pure fluids (though the data coverage is very heterogeneous; see below). Of those fluids, 2570 were included in our fit because they had sufficient experimental data coverage.

- *Direct fitting of experimental data*: Rather than fitting curve fitted pseudo-experimental data as in Le Guennec *et al.*, we have directly employed the experimental data of NIST TDE in our fitter.

- *Algorithm*: We provide comprehensive description of the fitting process and provide the source code used in our fitter. All parts of the fitting process use open-source tools and packages for cross-platform replicability.

2 Thermodynamic modeling

2.1 Cubic equations of state

The development of new cubic equations of state remains an active field of research,[9] as well as the extension of cubic equations of state with activity coefficient models.[7,10–14] One of the primary motivations for this work is to serve as a reference for the properties of the pure fluids in cubic + activity coefficient models such as those of the group-contribution volume-translated Peng-Robinson (VTPR)[12,15–19] equation or predictive Soave-Redlich-Kwong (PSRK).[7] Moreover, as demonstrated by Le Guennec et al.,[20] it is absolutely imperative to use a consistent α function when fitting only subcritical data and applying the model to supercritical states.

While a comprehensive analysis of the multitude of equations of state that are either direct descendants (or distant offspring) of the van der Waals equation of state is beyond the scope of this paper, we refer the interested reader to the literature for a further review.[9,21,22] In this study we focus on one of the cubic equations of state with the most significant present-day

influence – the Peng-Robinson[4,5] equation of state.

The most industrially relevant cubic equations of state can be given in the form[23]

$$p = \frac{RT}{v-b} - \frac{a(T)}{(v+\Delta_1 b)(v+\Delta_2 b)} \tag{1}$$

where Δ_1 and Δ_2 are constants that are set to yield the desired equation of state (see Bell and Jäger[24] or Michelsen[23] for more information). In the case of Peng-Robinson, $\Delta_1 = 1+\sqrt{2}$ and $\Delta_2 = 1-\sqrt{2}$, and in the case of Soave-Redlich-Kwong, $\Delta_1 = 1$ and $\Delta_2 = 0$. In addition, b is the co-volume, a is the attractive term, and v is the molar volume.

In the standard implementations of a cubic EOS, the attractive term a generally takes the form

$$a = a_0 \alpha(T_\mathrm{r}), \tag{2}$$

where a_0 is an constant of the form $a_0 = c_0 R^2 T_\mathrm{c}^2/p_\mathrm{c}$, and where c_0 is EOS-dependent. In the Peng-Robinson or Soave-Redlich-Kwong EOS the α function is given by the form

$$\alpha = \left[1 + m\left(1 - \sqrt{T/T_\mathrm{c}}\right)\right]^2 \tag{3}$$

as proposed by Soave and co-workers.[25] The parameter m is a function of the acentric factor of the fluid. The attractive term of Mathias & Copeman[26] is an extension of this general form. An alternative (and now preferred) form for the attractive function is that of Twu:[27]

$$\alpha = \left(\frac{T}{T_\mathrm{c}}\right)^{C_2(C_1-1)} \exp\left[C_0\left(1 - \left(\frac{T}{T_\mathrm{c}}\right)^{C_1 C_2}\right)\right]. \tag{4}$$

This form is now preferred[28] because the parameters C_0, C_1, and C_2 can be selected to meet some important consistency conditions that are difficult or impossible to enforce with other functional forms. These conditions are further described in Section 4.4.

A number of authors have attempted to develop generalized approaches for the attractive parameters for cubic EOS, with varying levels of success.[29] There have also been attempts to determine physical constraints on the terms in the cubic equation of state.[8,20,28,30,31]

2.2 Helmholtz transformations

In the state-of-the-art thermophysical property libraries, the equation of state is expressed in terms of non-dimensionalized Helmholtz energy $\alpha_\mathrm{e} = a_e/(RT)$ rather than in a pressure-explicit form. The Helmholtz energy a_e is a thermodynamic potential from which all other thermodynamic properties can be obtained. Therefore the EOS can be expressed as

$$\alpha_\mathrm{e}(\tau,\delta) = \alpha_\mathrm{e}^0(\tau,\delta) + \alpha_\mathrm{e}^\mathrm{r}(\tau,\delta), \tag{5}$$

where $\tau = T_\mathrm{r}/T$ and $\delta = \rho/\rho_\mathrm{r}$ are the reciprocal reduced temperature and the reduced density, respectively. The reducing temperature T_r and the reducing density ρ_r are usually, but not always, their values at the critical point.

The generalized non-dimensionalized residual Helmholtz energy contribution $\alpha_\mathrm{e}^\mathrm{r}$ can be given by[24]

$$\alpha_\mathrm{e}^\mathrm{r} = -\ln(1-b\delta\rho_\mathrm{r}) - \frac{\tau a}{RT_\mathrm{r}} \frac{\ln\left(\frac{\Delta_1 b\rho_\mathrm{r}\delta + 1}{\Delta_2 b\rho_\mathrm{r}\delta + 1}\right)}{b(\Delta_1 - \Delta_2)}. \tag{6}$$

As in Bell and Jäger,[24] Eq. (6) can be factored into the form

$$\alpha_\mathrm{e}^\mathrm{r} = \psi^{(-)}(\delta) - \frac{\tau a(\tau)}{RT_\mathrm{r}}\psi^{(+)}(\delta). \tag{7}$$

The ideal-gas contribution α_e^0 of the equation of state (see for instance Lemmon *et al.*[32]) is given by

$$\alpha_\mathrm{e}^0 = \frac{h_0^0\tau}{RT_c} - \frac{s_0^0}{R} - 1 + \ln\frac{\delta\tau_0}{\delta_0\tau} - \frac{\tau}{R}\int_{\tau_0}^{\tau}\frac{c_p^0}{\tau^2}\mathrm{d}\tau + \frac{1}{R}\int_{\tau_0}^{\tau}\frac{c_p^0}{\tau}\mathrm{d}\tau \tag{8}$$

where $\delta_0 = \rho_0/\rho_\mathrm{c}$, $\tau_0 = T_\mathrm{c}/T_0$, and c_p^0 is the ideal-gas specific heat capacity as a function of temperature (or reciprocal reduced temperature τ). The subscript "0" indicates that the property is for the reference state of the EOS. The ideal-gas contribution can also be written in the form $\alpha_\mathrm{e}^0 = \ln\delta + f(T)$ to highlight the separability of the temperature and density dependence of α_e^0.

3 Data curation and preparation

In this work we used the experimental data contained in the ThermoData Engine database (TDE).[33–36] This database contains a large body of experimental data (for nearly 24,000 pure fluids), and includes methods for critically evaluating the uncertainty and thermodynamic consistency of experimental data. We include in this study only experimental data that pass the critical evaluation checks of TDE.

The data were prepared by selecting all the pure fluids for which, at a minimum:

- Critical temperature data were available
- Saturation pressure data were available with at least 10 data points passing the critical evaluation tests; saturation pressures below $p_c/10^6$ or saturation temperatures above $0.8T_c$ were not included[1].

For some fluids, additional useful data were available in TDE, including critical pressure data, latent heat of vaporization data, triple-point temperature data, etc. For many fluids there is a significant paucity of experimental data; for some fluids, there are as few as one data point among all data types.

While the critical temperature is usually measured directly, the "experimentally measured" critical pressure given in literature is often evaluated by extrapolating the saturation pressure data to the measured critical temperature, for instance by fitting an Antoine-type equation to the saturation pressure versus temperature data and extrapolating to the given critical temperature to obtain the critical pressure. The critical pressure value calculated by TDE is used without modification.

The acentric factor ω appearing in the baseline equation of state forms for the Peng-Robinson and SRK equations is never measured directly, rather it is obtained as a post-processing step applied to the experimental data. The definition of the acentric factor is[21]

$$\omega = -\log_{10}\left(\frac{p_\sigma(0.7T_c)}{p_c}\right) - 1. \qquad (9)$$

Determination of the acentric factor from experimental data is a multi-step process:

1. Determine the critical temperature and pressure as described above.
2. Obtain a saturation pressure curve (from a functional form such as the Antoine equation) for the saturation pressure data, with the functional dependency $p_\sigma = f(T)$.
3. Evaluate the saturation pressure curve at $0.7T_c$, and evaluate the acentric factor from Eq. (9).

Figure 2 shows the data distribution for the pure fluids included in TDE that were used in this study. There are comparatively few fluids that have both a significant number of vapor pressure measurements and well as latent heat measurements. The bulk of the fluids are found in the domain with only a few vapor pressure measurements, and for many of those fluids, few (or no) latent heat measurements.

The metadata associated with each fluid is based on the InChI key of the fluid, a unique identifier based on the molecular connectivity information[2]. The InChI key is broadly understood by cheminformatics systems, and is unencumbered by intellectual property restrictions. CAS registry numbers, on the other hand, are proprietary information.

4 Algorithmic approach

4.1 Objective function

The objective function for this problem is the sum of the squared residues in the residue vector. Mathematically, our objective function is

[1] These points were rejected due to the numerical difficulties of carrying out vapor-liquid-equilibrium calculations at these states; derived vapor pressures for heavy linear alkanes are available at pressures below 10^{-20} Pa[37]

[2] Though useful for generating unique identifiers for nearly all compounds based on molecular connectivity information, the InChI string/key is not able to disambiguate spin isomers like ortho-, para-, or normal-hydrogen.

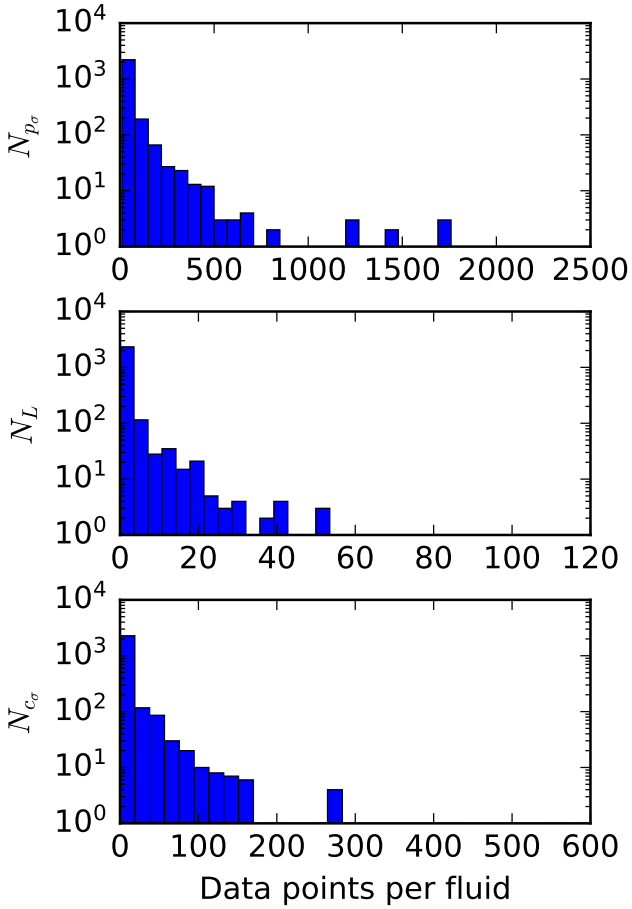

Figure 2: Distributions of the experimental data available for each data type for pure fluids in the NIST ThermoDataEngine. N_{p_σ}: number of fluids with this many experimental vapor pressure data points, N_L: number of fluids with this many latent heat of vaporization data points, N_{c_σ}: number of fluids with this many experimental saturation specific heat data points.

given by:

$$O(\vec{C}) = \sum_i (w_i r_i(\vec{C}))^2 \tag{10}$$

where each of the residue contributions $r_i = y_{\text{model},i} - y_{\text{exp},i}$ corresponds to a given data point (saturation pressure, latent heat, or saturation specific heat), as is described in the following sections, and as described in detail in the supplemental material. The parameters w_i weight the different property types, where a weight of one is used for the vapor pressure and latent heat of vaporization data, and a weight of 0.5 is used for the saturation specific heat data. These weights were obtained by experimentation to enforce the desired balance between the different properties. Within the properties, normalized weights as specified by the Thermodynamics Research Center were used to weight the data points.

The evaluation of the residues is an embarassingly parallel problem; each row in the residue vector can be evaluated entirely independently of the other rows. This creates a problem that is perfectly suited to parallel evaluation over several threads. In this case, we use the natively multithreaded C++11 library `NISTfit`[38] developed by the authors to evaluate the residues in parallel, yielding a nearly linear speedup versus purely serial evaluation. The `NISTfit` library also includes a thread-parallel implementation of the Levenberg-Marquardt sum of squares minimizer governed by a derivative-based trust region minimization. At the beginning of the fitting campaign, the Levenberg-Marquardt optimizer was used, and for that reason, analytic derivatives of each of the residues with respect to the coefficients were developed. These analytic derivatives are mathematically complex, and for that reason are presented in the supplemental material, where they are covered in detail.

One of the major disadvantages of Levenberg-Marquardt minimization is that there is no easy means of integrating nonlinear inequality constraints such as the consistency checks implemented in this paper. One of the most straightforward means of implementing inequality con-

straints in fitting is to use a nature-inspired evolutionary optimization technique in concert with penalty functions for the inequality constraints. There are numerous evolutionary-like optimization methods available in the literature, and the differential evolution[39] algorithm as implemented in the Python `scipy.optimize` package was used. Differential evolution operates by generating a large population of individuals (an individual is a set of Twu coefficients), and, for each individual, evaluating the cost function. Varying hybridization schemes are described in the literature for finding the lowest cost individual (best set of Twu coefficients).

The cost function for differential evolution is then given by

$$\mathrm{COST}(\vec{C}) = O(\vec{C}) + \mathrm{PENALTY}(\vec{C}) \quad (11)$$

where $\mathrm{PENALTY}(\vec{C})$ is the sum of the penalties for each constraint that is not satisfied. Each unfulfilled constraint added a large number (here, 1000) to the cost function. The differential evolution optimizer was then able to successfully carry out the global optimization problem within the domain specified by the constraints. Solutions not meeting the constraints were implicitly rejected by the optimizer. Differential evolution is a non-derivative-based optimization method and is therefore able to handle the discontinuities in the objective function caused by the constraints.

4.2 Constraints

As is described in Le Guennec *et al.*,[8,28] there are constraints on the Twu attractive parameters $\vec{C}$ that should be enforced in order to ensure reasonable outputs and extrapolation behavior from the equation of state. These constraints are that:

- α should be 1 at $T_\mathrm{r} = 1$.
- α should always be greater than zero.
- The derivative $\mathrm{d}\alpha/\mathrm{dT_r}$ should always be less than or equal to zero.
- The derivative $\mathrm{d}^2\alpha/\mathrm{dT_r^2}$ should always be greater than or equal to zero.
- The derivative $\mathrm{d}^3\alpha/\mathrm{dT_r^3}$ should always be less than or equal to zero.

Many authors that have developed sets of Twu attractive parameters have not enforced these constraints, yielding highly suspect extrapolation behavior outside the domain in which the parameters were fit.

Le Guennec *et al.*[28] gives the following two constraints, ***both*** of which MUST be enforced:
Constraint 1:

$$-\Delta \geq 0 \quad (12)$$

Constraint 2:

$$C_0\gamma \geq 0 \quad (13)$$

where $\Delta = C_2(C_1 - 1)$ and $\gamma = C_1C_2$.

In this case we express each constraint as the expression being greater than or equal to zero - this is the general form of the constraints required in many optimization routines. In each constraint, the left hand side is only a function of the attractive parameters $\vec{C}$.

There are furthermore two constraints (3a and 3b), ***at least one of which*** must be satisfied to ensure consistency.
Constraint 3a:

$$1 - \Delta - \gamma \geq 0 \quad (14)$$

Constraint 3b (both conditions must be met):

$$\begin{cases} 1 - 2\Delta + 2\sqrt{\Delta(\Delta - 1)} - \gamma \geq 0 \\ 4Y^3 + 4ZX^3 + 27Z^2 - 18XYZ - X^2Y^2 \geq 0 \end{cases} \quad (15)$$

where

$$X = -3(\gamma + \delta - 1) \quad (16)$$

$$Y = \gamma^2 + 3\delta\gamma - 3\gamma + 3\delta^2 - 6\delta + 2 \quad (17)$$

$$Z = -\delta(\delta^2 - 3\delta + 2) \quad (18)$$

A consistent set of Twu parameters is therefore one that satisfies constraints 1 and 2 and at least one of constraints 3a and 3b.

4.3 Residues

The residues used in this work are of three fundamental types:

1. *Saturation pressure*: Equality of the experimental saturation pressure with the model prediction is thermodynamically equivalent to the model-predicted Gibbs energy being the same in both phases for the experimental pressure. Therefore, the difference in Gibbs energy between the liquid and vapor phases, each evaluated at the experimental temperature and pressure, is driven to zero.

2. *Latent heat of vaporization*: The difference in latent heat of vaporization with the experimentally-measured value is driven to zero.

3. *Saturation specific heat*: The saturation specific heat can be experimentally measured at states where the measurement of the vapor pressure is difficult or impossible. Therefore, saturation specific heat data can provide useful information on the shape of the thermodynamic surface. As noted by Le Guennec *et al.*,[20] the inclusion of c_σ data is imperative to more fully constrain the behavior of the equation of state. One disadvantage of the use of saturation specific heat data is that a model for the ideal-gas specific heat of the fluid must be available. In this case, we used the fitted values for c_p^0 provided by the Wilhoit correlation coefficients available in TDE.

The residues are added together as described in Eq. (10). The analytic form of each residue is presented in the supplemental material, along with additional derivations required to implement each of the residue terms.

4.4 Implementation

For a given fluid, the following approach is employed:

1. The experimental data for a given fluid is retrieved from cached data obtained from NIST ThermoDataEngine.

2. If sufficient data are not available, the fluid is not included.

3. If sufficient data are available, the acentric factor is obtained by fitting an Antoine curve to the saturated pressure data over the entire temperature range, and is then evaluated according to Eq. (9). These values are only used to provide guess values for the saturation calls; thus, extremely precise acentric factors are not required.

4. Differential evolution is used to carry out the optimization in two parts:

   (a) Constraints 1, 2, and 3a are imposed, and the optimization is carried out. If the optimization terminates successfully, the result is stored.

   (b) Constraints 1, 2, and both parts of 3b are imposed, and the optimization is carried out. If the optimization terminates successfully, the result is stored.

5. The best individual from the optimization is retained. The output of this step is the final optimized value of the consistent Twu vector of coefficients $\vec{C}$.

The final minimization algorithm was implemented by hybridizing a number of open-source tools. The implementation of the generalized Helmholtz energy transformations of the cubic equations of state of Bell and Jäger[24] were used to evaluate the Helmholtz energy contributions found in the residues and the Jacobian matrix. Data input and output uses the standardized JSON (javascript object notation) file format for native interoperability between C++ and Python (or other high-level languages). In C++, the `rapidjson` library is used for JSON file input/output, and the `Eigen` library is used for the matrix math operations. Some computational routines (e.g., generic C++ routines

for nonlinear equation solving) have been taken from the CoolProp library.[40]

The C++ interface was wrapped into a module in the Python programming language through the use of the `pybind11`[41] package. The Python module retains the convenience of a high-level programming language while also achieving computational speeds commensurate with a low-level programming language (C++ in this case). The amount of shim code to construct the interface between C++ and Python is minimal; the `pybind11` templates carry out most of the datatype conversions.

The source code used to carry out the minimization is given in the supplemental material, as well as some artificial "experimental" data generated from the multiparameter equation of state of n-hexane[42] for testing purposes.

5 Results

We applied the fitting methodology described above to fit a consistent set of Twu attractive parameters for 2570 fluids and obtained the parameters given in the supplemental material. For each property, we define the average absolute deviation (AAD) as a percentage given as

$$\mathrm{AAD}_Y = \frac{100}{N}\sum_{i=1}^{N}\left|1 - \frac{Y_{\mathrm{calc},i}}{Y_{\mathrm{exp},i}}\right| \tag{19}$$

where Y is the property of interest (vapor pressure, latent heat, or saturation specific heat). If a calculated value is unable to be evaluated by the model (most especially at extremely low pressures), it is not included in the AAD.

Figures 3 to 5 show the coverage and error distributions for the saturation pressure, latent heat of vaporization, and saturation specific heat data for the fluids included in this fitting exercise. These figures give a high-level overview of the representation of the experimental data by the Peng-Robinson equation of state augmented by the Twu attractive function parameters obtained in this work. In each figure, a two-dimensional density plot is shown, and histograms show for the distributions in each of the two plotted variables, here the number of data points and the AAD in the representation of the given variable.

The average of the AAD of a property Y for all the fluids that have this property is defined by

$$\overline{\mathrm{AAD}}_Y = \mathrm{mean}(\overrightarrow{AAD_Y}) \tag{20}$$

results in the following values:

- $\overline{\mathrm{AAD}}_{p_\sigma} = 4.9\%$
- $\overline{\mathrm{AAD}}_{c_\sigma} = 0.9\%$
- $\overline{\mathrm{AAD}}_{L} = 1.5\%$

The AAD of the properties can vary over a few orders of magnitude. Therefore, the more relevant metric is the logarithm of the AAD. The log-average of the AAD of a property Y for all the fluids that have this property,

$$\overline{\log\mathrm{AAD}}_Y = \exp(\mathrm{mean}(\log(\overrightarrow{AAD_Y}))), \tag{21}$$

results in the following values for the properties under consideration:

- $\overline{\log\mathrm{AAD}}_{p_\sigma} = 2.05\%$
- $\overline{\log\mathrm{AAD}}_{c_\sigma} = 0.39\%$
- $\overline{\log\mathrm{AAD}}_{L} = 0.34\%$

These values correspond to the peaks of each of the histograms in AAD in Figures 3 to 5.

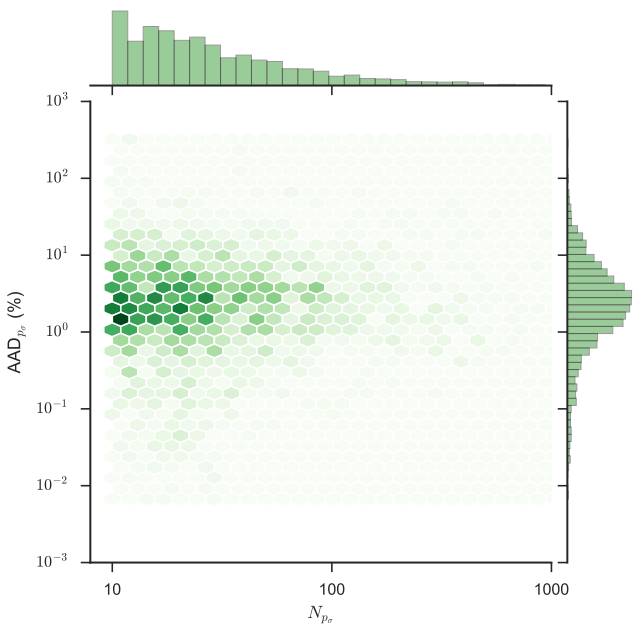

Figure 3: Distribution of the AAD error of saturation pressure from fitting Twu parameters and data point availability. The darker the hex, the more data points fall within it.

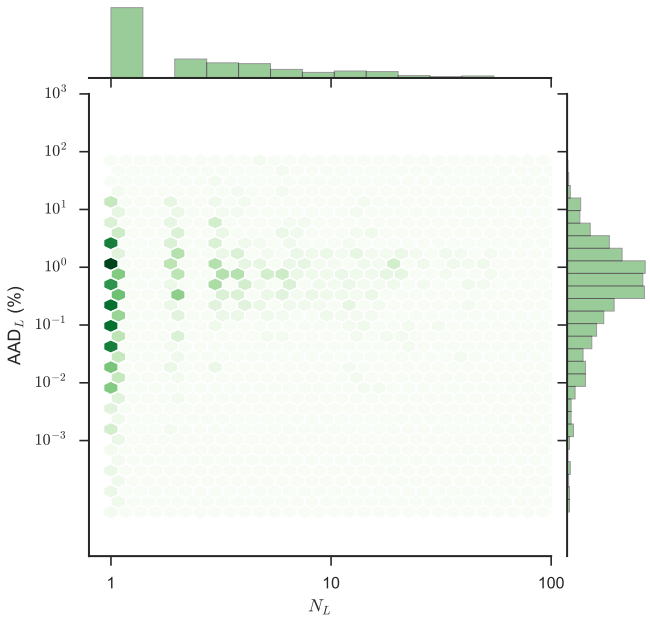

Figure 4: Distribution of the AAD error from fitting Twu parameters of latent heat of vaporization and data point availability. The darker the hex, the more data points fall within it.

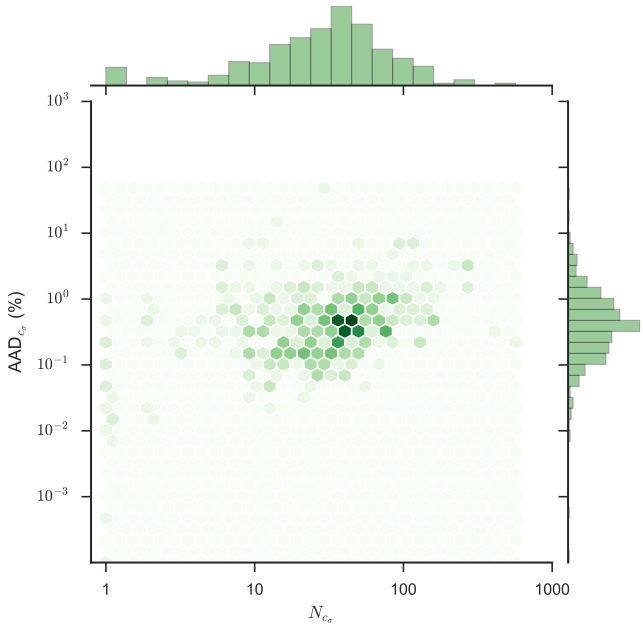

Figure 5: Distribution of the AAD error from fitting Twu parameters of saturation specific heat c_σ and data point availability. The darker the hex, the more data points fall within it.

An important check on the behavior of the fitted parameters is an assessment of the shape of the α function, as described in section 4.2 and in Le Guennec *et al.*[8,28] Therefore, the α functions were plotted for 50 illustrative fluids, selected by their sorted value of α at $T_\mathrm{r} = 0.2$. Figure 6 shows the results for high values of T_r, and Fig. 7 for low values of T_r, demonstrating by visual inspection that the curves all 1) pass through $(T_\mathrm{r}, \alpha) = (1, 1)$, 2) yield α values above zero, and 3) have negative slopes and positive second derivatives. Therefore, each of these α functions satisfy the conditions of consistency laid out by Le Guennec *et al.*;[8,28] this is as expected because the consistency constraints were imposed in the fitting procedure.

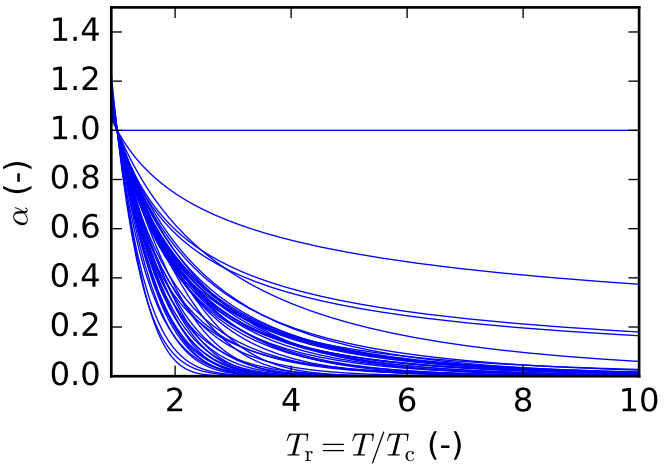

Figure 6: Plots of α as a function of T_r at high T_r for 50 illustrative fluids

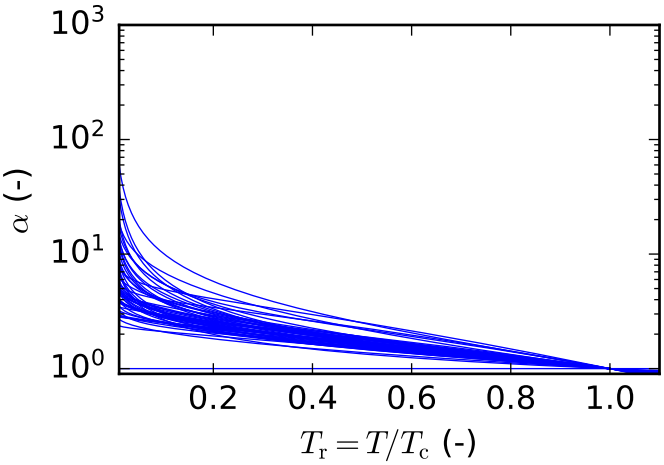

Figure 7: Plots of α as a function of T_r at low T_r for 50 illustrative fluids

The Waring number[43] (also known as Riedel's factor) is a property derivative that can be used to check that the shape of the vapor pressure curve is reasonable. For that reason, it can be instructive to plot the Waring number, given by

$$\mathrm{Wa} = -R\left(\frac{\partial(\ln p)}{\partial(1/T)}\right)_\sigma = \frac{RT^2}{p}\left(\frac{\partial p}{\partial T}\right)_\sigma, \quad (22)$$

as a function of reduced temperature T_r. While there are no hard-and-fast rules for the required shape of the curve of the Waring number, Waring[43] suggests that this number should have a minimum value at a T_r value of approximately 0.8 or 0.85, have positive second derivatives everywhere, and negative first derivatives for T_r less than the Wa minimum and positive first derivative for T_r greater than the Wa minimum. The Waring number is finite at the critical point (see for instance Wagner[44]). The Waring number is shown in Fig. 8 for the same fluids studied by Waring:[43] methane, ethane, propane, *n*-butane, *n*-pentane, *n*-heptane, ethylene, propylene, 1,3 butadiene, benzene, chlorodifluoromethane (refrigerant 13), methanol, carbon dioxide, carbon disulfide, sulfur dioxide, and ethylene oxide. The Waring numbers for all these fluids, when modeled with the α function from this work, demonstrate the qualitatively correct behavior.

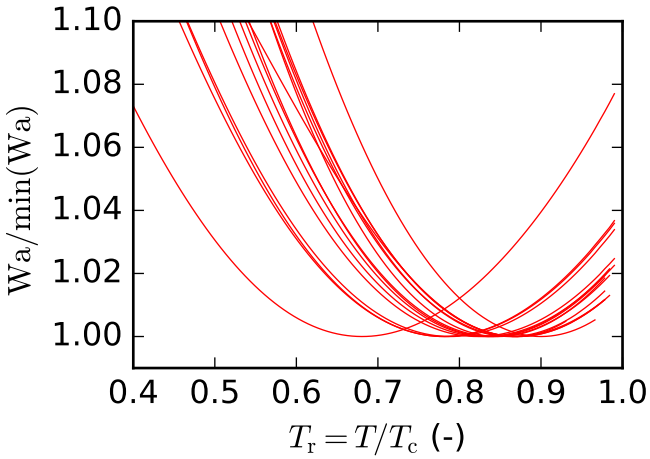

Figure 8: Plot of Waring numbers divided by its value at the minimum as a function of T_r for the fluids selected by Waring[43]

Another conclusion from this fitting exercise, as also noticed by Le Guennec et al.[8], is that the Peng-Robinson + Twu formulation is not always adequate for representing strongly interacting fluids (e.g., acids). As a particularly striking demonstration of the challenges inherent in representing the phase equilibria of strongly associating fluids, we present in Fig. 9 the data representation for both vapor pressure and latent heat for acetic acid. The AAD for the vapor pressure, when only the vapor pressure data are included in the fit, is 1.1%, whereas when the latent heat data and saturation specific heat data are included, the AAD in vapor pressure is more than 19%! For more weakly associating fluids, the challenges of rep-

resentation of the experimental data are much less severe. Even water, a strongly interacting fluid, has a vapor pressure AAD of 1.2% and a latent heat AAD of 1.0%. Thus, while we have endeavored to yield as accurate a representation of the phase equilibria that we can, users should be aware of the limitations of these parameters in representing the properties of strongly associating fluids; a healthy dose of caution is appropriate.

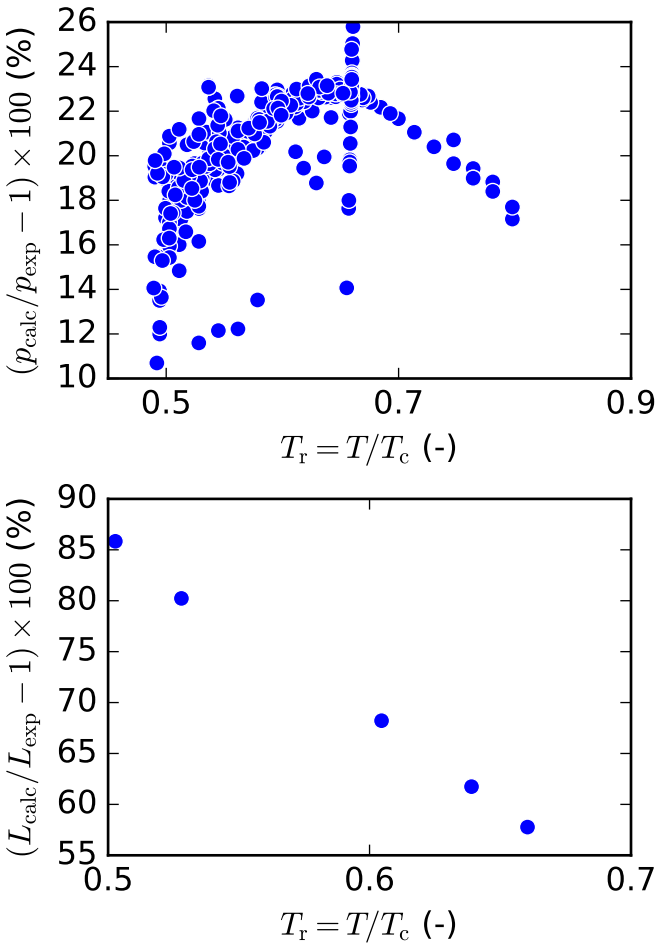

Figure 9: Deviations of the property predictions for acetic acid with the Twu coefficients as fit in this work

Conclusions

In this work we have developed a database of consistent α parameters for the Peng-Robinson equation of state. These parameters yield accurate representations of the thermodynamic properties of nearly 2600 fluids. A number of quantitative and qualitative assessments of the α function have been carried out, demonstrating that the α functions yield consistent, accurate, and reasonable behavior of the equation of state. This database of Twu α function parameters therefore forms the basis for the next generation of Peng-Robinson implementations.

Acknowledgement This article is dedicated to the memory of Marco Satyro, who tragically passed away while this work was underway. The authors thank 1) Romain Privat and Jean-Noël Jaubert of the Université de Lorraine, France for answering numerous questions about the consistency check and providing check values, 2) Vladimir Diky (of NIST) for bringing to our attention the Waring number, and discussions of fitting procedures, 3) Kenneth Kroenlein and Chris Muzny (both of NIST) for their assistance with data extraction from TDE, 4) Andreas Jäger of Technische Universität Dresden for assistance with the analytic derivatives.

References

(1) van der Waals, J. D. Over de Continuiteit van den Gas- en Vloeistoftoestand. Ph.D. thesis, University of Leiden, 1873.

(2) Trebble, M.; Bishnoi, P. Accuracy and consistency comparisons of ten cubic equations of state for polar and non-polar compounds. *Fluid Phase Equilib.* **1986**, *29*, 465–474, DOI: 10.1016/0378-3812(86)85045-2.

(3) Boshkova, O.; Deiters, U. Soft repulsion and the behavior of equations of state at high pressures. *Int. J. Thermophys.* **2010**, *31*, 227–252, DOI: 10.1007/s10765-010-0727-7.

(4) Peng, D.-Y.; Robinson, D. B. A New Two-Constant Equation of State. *Ind. Eng. Chem. Fundamen.* **1976**, *15*, 59–64, DOI: 10.1021/i160057a011.

(5) Robinson, D. B.; Peng, D.-Y. *The characterization of the heptanes and heavier fractions for the GPA Peng-Robinson programs (Research Report RR-28)*; Gas Processors Association, 1978.

(6) Wagner, W.; Pruß, A. The IAPWS Formulation 1995 for the Thermodynamic Properties of Ordinary Water Substance for General and Scientific Use. *J. Phys. Chem. Ref. Data* **2002**, *31*, 387–535, DOI: 10.1063/1.1461829.

(7) Horstmann, S.; Jabłoniec, A.; Krafczyk, J.; Fischer, K.; Gmehling, J. PSRK group contribution equation of state: comprehensive revision and extension IV, including critical constants and α-function parameters for 1000 components. *Fluid Phase Equilib.* **2005**, *227*, 157–164, DOI: 10.1016/j.fluid.2004.11.002.

(8) Le Guennec, Y.; Privat, R.; Jaubert, J.-N. Development of the translated-consistent tc-PR and tc-RK cubic equations of state for a safe and accurate prediction of volumetric, energetic and saturation properties of pure compounds in the sub- and super-critical domains. *Fluid Phase Equilib.* **2016**, *429*, DOI: 10.1016/j.fluid.2016.09.003.

(9) Valderrama, J. The State of the Cubic Equations of State. *Ind. Eng. Chem. Res.* **2003**, *42*, 1603–1618.

(10) Kontogeorgis, G. M.; Folas, G. K. *Thermodynamic Models for Industrial Applications: From Classical and Advanced Mixing Rules to Association Theories*; Wiley, 2010.

(11) Kontogeorgis, G. M.; Coutsikos, P. Thirty Years with EoS/G^E Models–What Have We Learned? *Ind. Eng. Chem. Res.* **2012**, *51*, 4119–4142, DOI: 10.1021/ie2015119.

(12) Ahlers, J.; Gmehling, J. Development of an universal group contribution equation of state. Prediction of liquid densities for pure compounds with a volume translated Peng-Robinson equation of state. *Fluid Phase Equilib.* **2001**, *191*, 177–188, DOI: 10.1016/S0378-3812(01)00626-4.

(13) Jaubert, J.-N.; Mutelet, F. VLE predictions with the Peng-Robinson equation of state and temperature dependent kij calculated through a group contribution method. *Fluid Phase Equilib.* **2004**, *224*, 285–304, DOI: http://dx.doi.org/10.1016/j.fluid.2004.06.05

(14) Qian, J.-W.; Privat, R.; Jaubert, J.-N. Predicting the Phase Equilibria, Critical Phenomena, and Mixing Enthalpies of Binary Aqueous Systems Containing Alkanes, Cycloalkanes, Aromatics, Alkenes, and Gases (N2, CO2, H2S, H2) with the PPR78 Equation of State. *Ind. Eng. Chem. Res.* **2013**, *52*, 16457–16490, DOI: 10.1021/ie402541h.

(15) Ahlers, J.; Gmehling, J. Development of a universal group contribution equation of state. 2. Prediction of vapor- liquid equilibria for asymmetric systems. *Ind. Eng. Chem. Res.* **2002**, *41*, 3489–3498.

(16) Ahlers, J.; Gmehling, J. Development of a universal group contribution equation of state III. Prediction of vapor- liquid equilibria, excess enthalpies, and activity coefficients at infinite dilution with the VTPR model. *Ind. Eng. Chem. Res.* **2002**, *41*, 5890–5899.

(17) Schmid, B.; Gmehling, J. Revised parameters and typical results of the VTPR group contribution equation of state. *Fluid Phase Equilib.* **2012**, *317*, 110–126, DOI: 10.1016/j.fluid.2012.01.006.

(18) Schmid, B.; Gmehling, J. Present status of the group contribution equation of state VTPR and typical applications for process development. *Fluid Phase Equilib.* **2016**, *425*, 443–450.

(19) Schmid, B.; Schedemann, A.; Gmehling, J. Extension of the VTPR group contribution equation of state: Group interaction parameters for additional 192 group combinations and typical results. *Ind. Eng. Chem. Res.* **2014**, *53*, 3393–3405, DOI: 10.1021/ie404118f.

(20) Le Guennec, Y.; Privat, R.; Lasala, S.; Jaubert, J.-N. On the imperative need to

use a consistent α-function for the prediction of pure-compound supercritical properties with a cubic equation of state. *Fluid Phase Equilib.* **2017**, *445*, 45–53, DOI: 10.1016/j.fluid.2017.04.015.

(21) Poling, B. E.; Prausnitz, J. M.; O'Connell, J. P. *The Properties of Gases and Liquids, 5th edition*; McGraw Hill, 2001.

(22) Wei, Y. S.; Sadus, R. J. Equations of State for the Calculation of Fluid-Phase Equilibria. *AIChE Journal* **2000**, *46*, 169–196.

(23) Michelsen, M. L.; Mollerup, J. M. *Thermodynamic Models: Fundamentals & Computational Aspects*; Tie-Line Publications, 2007.

(24) Bell, I. H.; Jäger, A. Helmholtz Energy Transformations of Common Cubic Equations of State for Use with Pure Fluids and Mixtures. *J. Res. NIST* **2016**, *121*, DOI: 10.6028/jres.121.011.

(25) Soave, G. Equilibrium Constants from a Modified Redlich-Kwong Equation of State. *Chem. Eng. Sci.* **1972**, *27*, 1197–1203, DOI: 10.1016/0009-2509(72)80096-4.

(26) Mathias, P. M.; Copeman, T. W. Extension of the Peng-Robinson equation of state to complex mixtures: evaluation of the various forms of the local composition concept. *Fluid Phase Equilib.* **1983**, *13*, 91–108.

(27) Twu, C. H.; Bluck, D.; Cunningham, J. R.; Coon, J. E. A cubic equation of state with a new alpha function and a new mixing rule. *Fluid Phase Equilib.* **1991**, *69*, 33 – 50, DOI: 10.1016/0378-3812(91)90024-2.

(28) Le Guennec, Y.; Lasala, S.; Privat, R.; Jaubert, J. N. A consistency test for alpha-functions of cubic equations of state. *Fluid Phase Equilib.* **2016**, *427*, 513–538, DOI: 10.1016/j.fluid.2016.07.026.

(29) Privat, R.; Visconte, M.; Zazoua-Khames, A.; Jaubert, J.-N.; Gani, R. Analysis and prediction of the alpha-function parameters used in cubic equations of state. *Chemical Engineering Science* **2015**, *126*, 584 – 603, DOI: 10.1016/j.ces.2014.12.040.

(30) Yelash, L. V.; Kraska, T. Investigation of a generalized attraction term of an equation of state and its influence on the phase behaviour. *Fluid Phase Equilib.* **1999**, *162*, 115 – 130, DOI: 10.1016/S0378-3812(99)00205-8.

(31) Cachadiña, I.; Mulero, A. On the range of applicability of the Carnahan-Starling-Patel-Teja equation of state. *Fluid Phase Equilib.* **2012**, *319*, 16 – 22, DOI: 10.1016/j.fluid.2012.01.027.

(32) Lemmon, E. W.; McLinden, M. O.; Wagner, W. Thermodynamic Properties of Propane. III. A Reference Equation of State for Temperatures from the Melting Line to 650 K and Pressures up to 1000 MPa. *J. Chem. Eng. Data* **2009**, *54*, 3141–3180, DOI: 10.1021/je900217v.

(33) Diky, V.; Chirico, R. D.; Muzny, C. D.; Kazakov, A. F.; Kroenlein, K.; Magee, J. W.; Abdulagatov, I.; Kang, J. W.; Frenkel, M. ThermoData Engine (TDE) software implementation of the dynamic data evaluation concept. 7. Ternary mixtures. *J. Chem. Inf. Model.* **2011**, *52*, 260–276, DOI: 10.1021/ci200456w.

(34) Frenkel, M.; Chirico, R. D.; Diky, V.; Yan, X.; Dong, Q.; Muzny, C. ThermoData Engine (TDE): software implementation of the dynamic data evaluation concept. *J. Chem. Inf. Model.* **2005**, DOI: 10.1021/ci050067b.

(35) Diky, V.; Chirico, R. D.; Muzny, C. D.; Kazakov, A. F.; Kroenlein, K.; Magee, J. W.; Abdulagatov, I.; Kang, J. W.; Gani, R.; Frenkel, M. ThermoData Engine (TDE): Software

implementation of the dynamic data evaluation concept. 8. Properties of material streams and solvent design. *J. Chem. Inf. Model.* **2012**, *53*, 249–266, DOI: 10.1021/ci300470t.

(36) Diky, V.; Chirico, R. D.; Muzny, C. D.; Kazakov, A. F.; Kroenlein, K.; Magee, J. W.; Abdulagatov, I.; Frenkel, M. ThermoData Engine (TDE): Software implementation of the dynamic data evaluation concept. 9. Extensible thermodynamic constraints for pure compounds and new model developments. *J. Chem. Inf. Model.* **2013**, *53*, 3418–3430, DOI: 10.1021/ci4005699.

(37) Chickos, J.; Wang, T.; Sharma, E. Hypothetical Thermodynamic Properties: Vapor Pressures and Vaporization Enthalpies of the Even n-Alkanes from C40 to C76 at T = 298.15 K by Correlation–Gas Chromatography. Are the Vaporization Enthalpies a Linear Function of Carbon Number? *J. Chem. Eng. Data* **2008**, *53*, 481–491, DOI: 10.1021/je7005852.

(38) Bell, I. H.; Kunick, M. NISTfit: A natively multithreaded C++11 framework for model development. *J. Res. NIST* **2017, submitted**,

(39) Storn, R.; Price, K. Differential Evolution – A Simple and Efficient Heuristic for global Optimization over Continuous Spaces. *J. Global Opt.* **1997**, *11*, DOI: 10.1023/A:1008202821328.

(40) Bell, I. H.; Wronski, J.; Quoilin, S.; Lemort, V. Pure and Pseudo-pure Fluid Thermophysical Property Evaluation and the Open-Source Thermophysical Property Library CoolProp. *Ind. Eng. Chem. Res.* **2014**, *53*, 2498–2508, DOI: 10.1021/ie4033999.

(41) Jakob, W.; Rhinelander, J.; Moldovan, D. pybind11 – Seamless operability between C++11 and Python. 2016; https://github.com/pybind/pybind11.

(42) Span, R.; Wagner, W. Equations of State for Technical Applications. II. Results for Nonpolar Fluids. *Int. J. Thermophys.* **2003**, *24*, 41–109, DOI: 10.1023/A:1022310214958.

(43) Waring, W. Form of a wide-range vapor pressure equation. *Industrial & Engineering Chemistry* **1954**, *46*, 762–763, DOI: 10.1021/ie50532a042.

(44) Wagner, W. New vapour pressure measurements for argon and nitrogen and a new method for establishing rational vapour pressure equations. *Cryogenics* **1973**, *13*, 470–482, DOI: 10.1016/0011-2275(73)90003-9.

Graphical TOC Entry